

A complete non-perturbative renormalization prescription for quasi-PDFs

Constantia Alexandrou^{a,b}, Krzysztof Cichy^{c,d}, Martha Constantinou^e,
Kyriakos Hadjyiannakou^b, Karl Jansen^f, Haralambos Panagopoulos^a, Fernanda Steffens^f

December 14, 2024

^a *Department of Physics, University of Cyprus, POB 20537, 1678 Nicosia, Cyprus*

^b *The Cyprus Institute, 20 Kavafi Str., Nicosia 2121, Cyprus*

^c *Goethe-Universität Frankfurt am Main, Institut für Theoretische Physik, Max-von-Laue-Strasse 1, 60438 Frankfurt am Main, Germany*

^d *Faculty of Physics, Adam Mickiewicz University, Umultowska 85, 61-614 Poznań, Poland*

^e *Department of Physics, Temple University, Philadelphia, PA 19122 - 1801, USA*

^f *John von Neumann Institute for Computing (NIC), DESY, Platanenallee 6, 15738 Zeuthen, Germany*



Abstract

In this work we present, for the first time, the non-perturbative renormalization for the unpolarized, helicity and transversity quasi-PDFs, in an RI' scheme. The proposed prescription addresses simultaneously all aspects of renormalization: logarithmic divergences, finite renormalization as well as the linear divergence which is present in the matrix elements of fermion operators with Wilson lines. Furthermore, for the case of the unpolarized quasi-PDFs, we describe how to eliminate the unwanted mixing with the twist-3 scalar operator.

We utilize perturbation theory for the one-loop conversion factor that brings the renormalization functions to the $\overline{\text{MS}}$ -scheme at a scale of 2 GeV. We also explain how to improve the estimates on the renormalization functions by eliminating lattice artifacts. The latter can be computed in one-loop perturbation theory and to all orders in the lattice spacing.

We apply the methodology for the renormalization to an ensemble of twisted mass fermions with $N_f=2+1+1$ dynamical light quarks, and a pion mass of around 375 MeV.

1 Introduction

Parton distribution functions (PDFs) describe the inner dynamics of partons inside a hadron [1]. They have a non-perturbative nature and, thus, they can not be computed in perturbation theory. Lattice QCD is an ideal formulation to study the PDFs from first principles, in large scale simulations. However, PDFs are usually defined on the light cone, which poses a problem for the standard Euclidean formulation. Hence, hadron structure calculations in lattice QCD are related to other quantities that are accessible in a Euclidean spacetime. This led to a long history of investigations of Mellin moments of PDFs and nucleon form factors (see [2, 3, 4, 5, 6] for recent reviews). In practice, there are severe limitations in the reconstruction of the PDFs mainly due to the small signal-to-noise ratio for the high moments. In addition, there are inevitable problems with power divergent mixings with lower dimensional operators. Therefore, the task of reconstructing the PDFs from their moments is practically unfeasible.

Ab initio evaluations of PDFs are of high importance as they would be a stringent test of non-perturbative aspects of QCD. The fact that a calculation of the PDFs from first principles is missing, is a pressing problem that prevents a deeper understanding of the nucleon structure. Our current knowledge on the PDFs relies on phenomenological fits from experimental data using perturbation theory. These parameterized PDFs serve, for example, as input for the computation of cross sections used for presently running colliders, most notably the LHC, and also to plan future collider experiments which are themselves tests of the Standard Model. The parameterizations are, however, not without ambiguities [7]. In addition, there are kinematical regions that are not experimentally accessible. The large Bjorken x region is one of them, with large uncertainties most dramatically seen in the down quark distributions [8, 9]. The transversity PDF is yet another example of a PDF that is only poorly constrained by phenomenology.

A pioneering method for a direct computation has been suggested by X. Ji [10]. In this approach, instead of matrix elements defined on the light cone, one calculates only local matrix elements of fermion operators including a finite-length Wilson line, and whose Fourier transform defines the so-called quasi-PDFs. This is achieved by taking the Wilson line in a purely spatial direction, conventionally chosen to be the z -direction, instead of the $+$ -direction on the light cone. In terms of hadron kinematics, the nucleon momentum is usually taken along this spatial direction. At large, but finite momenta, the quasi-PDFs can then be related to the light-front PDFs via a matching procedure [11, 12]. Ji's approach has already been tested in Refs. [13, 14, 15, 16, 17] and all these results are promising, i.e. they give a correct shape of the PDFs after the matching procedure. Certain properties of quasi-PDFs, like the nucleon mass dependence and target mass effects, have also been analyzed via their relation with transverse momentum dependent distribution functions (TMDs) [18, 19]. Nevertheless, the matrix elements of quasi-PDFs contain divergences that need to be eliminated via renormalization in order to obtain meaningful results that can be compared to the physical PDFs.

To date, all works on the quasi-PDFs only considered the bare matrix elements, as the renormalization process is highly non-trivial and was not addressed until recently. In particular, new complications arise in the renormalization of the Wilson line operators, compared to the local operators. For one, in addition to the logarithmic divergences there is a linear divergence [20] with respect to the lattice regulator, a , that prohibits one to take the continuum limit prior to its elimination. To one-loop level in perturbation theory the divergence is manifesting itself as a linear divergence, computed in Ref. [21] for a variety of fermion and gluon actions. However, it is of utmost importance to extract the power divergence non-perturbatively, which is one of the goals of this paper. Another feature of these operators that brings in new complications is the fact that certain choices of the Dirac structure exhibit mixing [21].

To show that these matrix elements can be renormalized, in particular that the linear divergence associated with the Wilson line can be eliminated, is of paramount importance. Without renormalization, the whole quasi-PDF strategy is incomplete and unable to provide any useful information to the theoretical and experimental community. Some suggestions for the elimination of the linear divergence via the static potential were proposed in Refs. [22, 23]. In Ref. [12] a one loop calculation of the linear divergence has been made, and that motivated the definition of an improved quasi-PDF that is free of power divergences. One has, nevertheless, to show that such a procedure can be done non-perturbatively. Another method to extract the coefficient of the linear divergence using the nucleon matrix elements of the quasi-PDFs was also presented in Ref. [21]. An alternative technique to suppress the linear divergence is discussed in Ref. [24] utilizing the gradient flow.

In this paper we propose, for the first time, a concrete renormalization method of the quasi-PDFs in a fully non-perturbative manner. We provide the prescription of the method and show examples of the renormalized matrix elements. We also discuss the elimination of the mixing between the unpolarized quasi-PDF and the twist-3 scalar operator. We employ the RI' renormalization scheme [25] and we convert the results to the $\overline{\text{MS}}$ scheme at a reference scale, $\bar{\mu} = 2 \text{ GeV}$, using the one-loop conversion factor computed in Ref. [21]. As a test case, we focus on the helicity quasi-PDFs to demonstrate results, as it is free of mixing. The outline of the paper is as follows: In Section 2 we provide the theoretical setup related to the nucleon matrix elements and the renormalization prescription in the presence and absence of mixing, as well as the data on the conversion factor computed perturbatively. Section 3 includes results on the renormalization functions, and we show the renormalized matrix elements for the helicity case. A discussion on the systematic uncertainties related to the renormalization is also provided. Finally we conclude and give our future directions.

2 Theoretical setup

In this section we briefly introduce the nucleon matrix elements for the quasi-PDFs that we aim to renormalize. We also explain the renormalization prescription for the three types of PDFs: unpolarized, helicity and transversity. For details on the computation of the nucleon matrix elements please see Refs. [15, 17].

2.1 Nucleon Matrix Elements

We consider matrix elements of non-local fermion operators that contain a straight Wilson line, denoted by $h_\Gamma(P_3, z)$. The variable z is the length of the Wilson line, and P_3 is the nucleon momentum, which is taken in the same direction as the Wilson line. The quasi-PDFs can be computed from the Fourier transformation of the following local matrix elements:

$$h_\Gamma(P_3, z) = \langle N | \bar{\psi}(0, z) \Gamma W_3(z) \psi(0, 0) | N \rangle, \quad (1)$$

where $|N\rangle$ is a nucleon state with spatial momentum $\vec{P}=(0, 0, P_3)$ along the 3-direction and $W_3(z)$ is a Wilson line of length z in the same direction. Γ denotes the Dirac structure of the operator insertion, which is γ_μ (unpolarized), $\gamma_\mu \cdot \gamma_5$ (helicity), $\sigma_{\mu\nu}$ (transversity). In the works appearing in the literature γ_μ is taken along the Wilson line. In principle, one may choose γ_μ orthogonal to the direction of the Wilson line. In this case, the unpolarized operator is free of mixing, while the helicity and transversity do mix. Our recent work [21] indicate that $\vec{P}_3 \perp \vec{z}$ ($\vec{P}_3 \parallel \vec{z}$) is ideal for the unpolarized (helicity and transversity) case.

To calculate the bare matrix elements, we use the setup of Ref. [17]. We consider one ensemble of dynamical $N_f=2+1+1$ twisted mass fermions produced by ETMC [26], with volume $32^3 \times 64$, lattice spacing $a \approx 0.082$ fm [27] and a bare twisted mass of $a\mu=0.0055$, which corresponds to a pion mass of around 375 MeV. We performed our calculations on 1000 gauge configurations with 15 forward propagators and 2 stochastic propagators, i.e. 30000 measurements in total. We will present results for momentum $P_3 = \frac{6\pi}{L}$, which is around 1.4 GeV in physical units. Gaussian smearing has been employed on the nucleon interpolating fields in the calculation of the matrix elements [17].

2.2 Renormalization Scheme

Here we discuss a fully non-perturbative renormalization prescription that will remove all divergences inherited in the matrix elements of the quasi-PDFs, as well as the mixing, as indicated in the perturbative analysis of Ref. [21]. In a nutshell, the proposed renormalization program:

- 1 removes the linear divergence that resums into a multiplicative exponential factor, $e^{-\delta m|z|/a+c|z|}$. The coefficient δm represents the strength of the divergence and is expected to be operator independent, as it is related only to the Wilson line. c is an arbitrary scale [28] that can be fixed by such a renormalization prescription;
- 2 takes away the logarithmic divergence with respect to the regulator, $\log(a\bar{\mu}_0)$, where $\bar{\mu}_0$ is the RI' renormalization scale;
- 3 applies the necessary finite renormalization related to the lattice regularization;
- 4 eliminates the mixing that appears in the unpolarized operator, as the bare matrix element is a linear combination of the unpolarized quasi-PDF and the twist-3 scalar operator. The two may be disentangled by the construction of a 2×2 mixing matrix.

We adopt a renormalization scheme which is applicable non-perturbatively, that is, the RI' scheme [25]. We compute vertex functions of the operators under study, between external quark states, with the setup being in momentum space, and the operator defined as:

$$\mathcal{O}_\Gamma = \bar{u}(x) \Gamma \mathcal{P} e^{ig \int_0^z A(\zeta) d\zeta} d(x + z\hat{\mu}), \quad (2)$$

where $\Gamma = \gamma_\mu, \gamma_\mu \cdot \gamma_5, \sigma_{\mu\nu}$ ($\nu \neq \mu$). The path ordering of the exponential appearing in the above expression becomes, on the lattice, a series of path ordered gauge links. The renormalization functions (Z-factors) depend on the length of the Wilson line and, thus, we perform a separate calculation for each value of z . Typically, z goes up to half of the spatial extent of the lattice.

The renormalization prescription is along the lines of the program developed for local operators and the construction of the vertex functions is described in detail in Ref. [29]. The main difference between the renormalization of the local operators and the Wilson-line operators is the linear divergence that appears in the latter case. However, there is no need to separate this divergence from the multiplicative renormalization function and, therefore, the technique described below may successfully extract both contributions at once.

Helicity and transversity quasi-PDFs

We will first provide the methodology for a general operator with a Wilson line in the absence of any mixing, which is applicable for the helicity and transversity quasi-PDFs. The

renormalization functions of the Wilson-line operators, $Z_{\mathcal{O}}$, are extracted by imposing the following conditions:

$$Z_q^{-1} Z_{\mathcal{O}}(z) \frac{1}{12} \text{Tr} \left[\mathcal{V}(p, z) (\mathcal{V}^{\text{Born}}(p, z))^{-1} \right] \Big|_{p^2 = \bar{\mu}_0^2} = 1, \quad (3)$$

where Z_q is the renormalization function of the quark field obtained via

$$Z_q = \frac{1}{12} \text{Tr} \left[(S(p))^{-1} S^{\text{Born}}(p) \right] \Big|_{p^2 = \bar{\mu}_0^2}. \quad (4)$$

The trace is taken over spin and color indices, and the momentum p entering the vertex function is set to the RI' renormalization scale $\bar{\mu}_0$. In Eq. (3) $\mathcal{V}(p, z)$ is the amputated vertex function of the operator and $\mathcal{V}^{\text{Born}}$ is its tree-level value, i.e. $\mathcal{V}^{\text{Born}}(p, z) = i\gamma_3\gamma_5 e^{ipz}$ for the helicity operator. Also, $S(p)$ is the fermion propagator and $S^{\text{Born}}(p)$ is the tree-level propagator. The RI' scale $\bar{\mu}_0$ is chosen such that its z -component is the same as the momentum of the nucleon. We test both diagonal (democratic) and parallel momenta to the Wilson line (in the spatial direction), that is $\vec{\mu}_0 = \frac{2\pi}{L} (P_3, P_3, P_3)$ and $\vec{\mu}_0 = \frac{2\pi}{L} (0, 0, P_3)$, respectively. We will refer to these choices as “diagonal” and “parallel”. The latter are expected to have larger lattice artifacts, as the ratio $\hat{P} \equiv \frac{\sum_{\rho} \bar{\mu}_{0\rho}^4}{(\sum_{\rho} \bar{\mu}_{0\rho}^2)^2}$ is higher than for diagonal momenta. Using renormalization scales leading to a small value for such a ratio has been successful for the local fermion operators [30, 29].

The vertex functions $\mathcal{V}(p)$ contain the same linear divergence as the nucleon matrix elements. This is crucial as it allows the extraction of the exponential together with the multiplicative Z -factor, through the renormalization condition of Eq. (3). More precisely, $Z_{\mathcal{O}}$ can be factorized as

$$Z_{\mathcal{O}}(z) = \bar{Z}_{\mathcal{O}} e^{+\delta m|z|/a - c|z|}, \quad (5)$$

where $\bar{Z}_{\mathcal{O}}$ is the multiplicative Z -factor of the operator and δm is the strength of the linear divergence. The exponential includes a term with an arbitrary scale c that could be of the form $c|z|$. Note that the exponential comes with a different sign compared to the nucleon matrix element. This is due to the fact that $Z_{\mathcal{O}}$ is related to the inverse of the vertex function, that is

$$Z_{\mathcal{O}} = \frac{Z_q}{\frac{1}{12} \text{Tr} \left[\mathcal{V}(p) (\mathcal{V}^{\text{Born}}(p))^{-1} \right] \Big|_{p=\bar{\mu}}}. \quad (6)$$

Such a construction of the Z -factor justifies the reason why the elimination of the power divergence in the nucleon matrix elements is successful by multiplying with $Z_{\mathcal{O}}$, provided that it has been calculated on the same ensemble. Consequently, the above renormalization condition handles all the divergences which are present in the matrix element under consideration. Note that in the absence of a Wilson line ($z=0$), the renormalization functions reduce to the local currents, free of any power divergence. For example, for the helicity operator, $Z_{\mathcal{O}}(z=0) \equiv Z_A$, the standard Z -factor of the axial current.

We would like to point out that knowledge of the value for the linear divergence coefficient, δm , provides insight on the strength of the power divergence. One can pursue this direction via the static potential [23] or the technique proposed in Ref. [21]. If the linear divergence is extracted, one may apply the matching of Ref. [12], which includes the coefficient δm . However, there is still a necessity to compute the multiplicative Z -factor to cure any logarithmic divergences, apply finite renormalization, as well as fix the arbitrary scale c .

Unpolarized quasi-PDFs

The case of the unpolarized quasi-PDFs requires special treatment, as it was demonstrated in Ref. [21] that there is a mixing with the twist-3 scalar operator. We establish notation by using the subscripts S and V for the scalar and vector (unpolarized) operators, respectively. The corresponding operators are:

$$\mathcal{O}_S = \bar{u}(x) \hat{1} \mathcal{P} e^{i g \int_0^z A(\zeta) d\zeta} d(x + z \hat{\mu}), \quad (7)$$

$$\mathcal{O}_V = \bar{u}(x) \gamma_\mu \mathcal{P} e^{i g \int_0^z A(\zeta) d\zeta} d(x + z \hat{\mu}), \quad (8)$$

and we represent their nucleon matrix elements as $h_S(P_3, z)$ and $h_V(P_3, z)$. To disentangle the two contributions from their bare matrix elements, one must compute the multiplicative renormalization and mixing coefficients from the following 2×2 matrix:

$$\begin{pmatrix} \mathcal{O}_V^R(P_3, z) \\ \mathcal{O}_S^R(P_3, z) \end{pmatrix} = \hat{Z}(z) \cdot \begin{pmatrix} \mathcal{O}_V(P_3, z) \\ \mathcal{O}_S(P_3, z) \end{pmatrix}, \quad (9)$$

where \hat{Z} is the matrix of the mixing pattern between the scalar and vector operators, that is

$$\hat{Z}(z) = \begin{pmatrix} Z_{VV}(z) & Z_{VS}(z) \\ Z_{SV}(z) & Z_{SS}(z) \end{pmatrix}. \quad (10)$$

According to the above mixing, the renormalized unpolarized quasi-PDF, $h_V^R(P_3, z)$, is related to the bare scalar and unpolarized via:

$$h_V^R(P_3, z) = Z_{VV}(z) h_V(P_3, z) + Z_{VS}(z) h_S(P_3, z), \quad (11)$$

where Z_{VV} and Z_{VS} are computed in a certain scheme. In the present work we employ the RI' scheme and then convert to the $\overline{\text{MS}}$, at an energy scale $\bar{\mu}$. The Z_{ii} factors can be computed following a prescription similar to Eq. (3), that is:

$$Z_q^{-1} \hat{Z}(z) \hat{\mathcal{V}}(p, z) \Big|_{p=\bar{\mu}} = \hat{1}, \quad (12)$$

where the elements of the vertex function matrix $\hat{\mathcal{V}}$ are given by the trace

$$\left(\hat{\mathcal{V}}(z) \right)_{ij} = \frac{1}{12} \text{Tr} \left[\mathcal{V}_i(p, z) (\mathcal{V}_j^{\text{Born}}(p, z))^{-1} \right], \quad i, j = S, V. \quad (13)$$

In the above equation $\mathcal{V}_i^{\text{Born}}$ is the tree-level expression of the operator \mathcal{O}_i . Thus, all matrix elements of \hat{Z} can be extracted by a set of linear equations, which can be written in the following matrix form:

$$Z_q^{-1} \begin{pmatrix} Z_{VV}(z) & Z_{VS}(z) \\ Z_{SV}(z) & Z_{SS}(z) \end{pmatrix} \cdot \begin{pmatrix} (\hat{\mathcal{V}}(z))_{VV} & (\hat{\mathcal{V}}(z))_{SV} \\ (\hat{\mathcal{V}}(z))_{VS} & (\hat{\mathcal{V}}(z))_{SS} \end{pmatrix} = \begin{pmatrix} 1 & 0 \\ 0 & 1 \end{pmatrix}. \quad (14)$$

As can be seen from Eq. (11), a major component in the renormalization of the unpolarized quasi-PDFs is knowledge of the scalar nucleon matrix element $h_S(P_3, z)$. To date, no lattice calculation is available for $h_S(P_3, z)$, as a mixing was not anticipated prior the work of Ref. [21]. Therefore, a proper renormalization of the unpolarized quasi-PDFs is still pending. However, the mixing appears to be greatly suppressed in the presence of a clover term in the fermionic action. This is of high importance, as we are currently computing the quasi-PDFs on an ensemble of twisted mass clover improved fermions at the physical pion mass [31, 32].

2.3 Conversion to the $\overline{\text{MS}}$ -scheme

The fermion operators with a finite-length Wilson line are scheme and scale dependent. As a result, having obtained the Z -factors in the RI' scheme as depicted in Eqs. (3) and (12) at the scale $\bar{\mu}_0$, we must convert them to the $\overline{\text{MS}}$ scheme at a scale $\bar{\mu}$. This conversion factor has been computed in one-loop continuum perturbation theory in Ref. [21]. In addition, comparison with phenomenological estimates is done typically at $\bar{\mu}=2$ GeV. The evolution of the scale requires the anomalous dimension of the operator, which is also known to one loop from the aforementioned work, and is given by

$$\gamma_{\mathcal{O}} = -3 \frac{g^2 C_f}{16\pi^2}. \quad (15)$$

Note that to one-loop level, the anomalous dimension does not depend on the Dirac structure of the operator and is the same in the RI' and $\overline{\text{MS}}$ schemes. The evolution to the $\overline{\text{MS}}$ renormalization scale $\bar{\mu}=2$ GeV is performed using the intermediate Renormalization Group Invariant scheme (RGI), as employed in Refs. [33, 34].

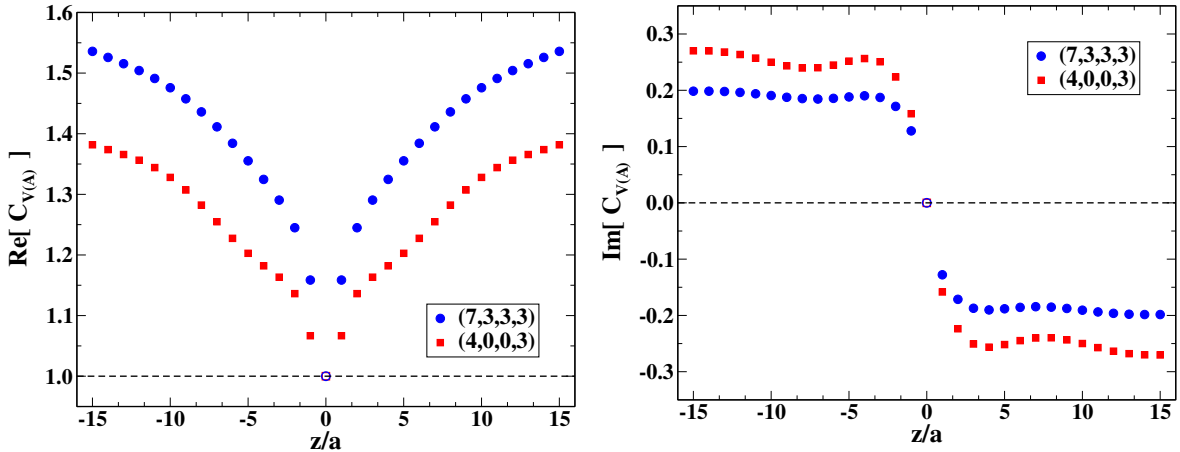


Figure 1: One-loop conversion factor from the RI' to the $\overline{\text{MS}}$ scheme. In the left (right) plot we show the real (imaginary) part of the conversion factor as a function of the length of the Wilson line in lattice units. The $\overline{\text{MS}}$ scale is set to $\bar{\mu}=2$ GeV. Two choices of the RI' scale have been employed: $\bar{\mu}_0=\frac{2\pi}{32}(\frac{7}{2}+\frac{1}{4}, 3, 3, 3)$ (blue circles) and $\bar{\mu}_0=\frac{2\pi}{32}(\frac{4}{2}+\frac{1}{4}, 0, 0, 3)$ (red squares). We use the abbreviation (7,3,3,3) and (4,0,0,3) in the legends, respectively.

As discussed in the previous Section, we employ two types of the RI' renormalization scale regarding the spatial direction: one the same as in the nucleon matrix elements, $\vec{\mu}_0=\frac{2\pi}{L}(0, 0, P_3)$, (parallel to the Wilson line direction), and one which is diagonal and each direction has a value of P_3 , that is $\vec{\mu}_0=\frac{2\pi}{L}(P_3, P_3, P_3)$. The conversion factor depends on both the RI' and $\overline{\text{MS}}$ renormalization scales. While $\bar{\mu}$ is fixed to 2 GeV, $\bar{\mu}_0$ can change affecting the numerical values of the conversion factor. This is illustrated in Fig. 1 for the unpolarized and helicity cases, which share the same conversion factor¹. We focus on the renormalization of the matrix elements with the nucleon boosted by $P_3=\frac{6\pi}{L}$, and we apply the same to the conversion factor, for the two cases of the renormalization scale. For the specific value of P_3 , we choose the temporal direction of $\bar{\mu}_0$ such that the ratio \hat{P} defined above, is as small as possible in order to suppress

¹The one-loop calculation does not depend on the prescription which one adopts for extending γ_5 to D dimensions (see, e.g., Refs. [35, 36, 37, 38, 39, 40] for a discussion of four relevant prescriptions and some conversion factors among them).

lattice artifacts. Nevertheless, for the “parallel” case the minimum value for the ratio is $\hat{P}=0.5$ which is already very high. The chosen values for $\bar{\mu}_0$ are: $\frac{2\pi}{32}(\frac{7}{2}+\frac{1}{4}, 3, 3, 3)$ and $\frac{2\pi}{32}(\frac{4}{2}+\frac{1}{4}, 0, 0, 3)$ for the “diagonal” and “parallel” case, respectively.

The real and imaginary parts of the conversion factor are plotted as a function of the length of the Wilson line, z . We stress that the dependence of the conversion factor on the renormalization scales and the length of the Wilson line is highly non-trivial and is expressed in terms of integrals of modified Bessel functions. Consequently, the data points shown in Fig. 1 have been computed numerically for the specific scales, at each value of z separately. We observe that the real part of the conversion is an order of magnitude larger than the imaginary part. The real part consistently increases for increasing values of z , while the imaginary part almost immediately stabilizes when z becomes non-zero. Also, the conversion factor at $z=0$ is equal to unity, as it correspond to the local vector and axial currents. Note that the case $z=0$ is not extracted from the calculation of Ref. [21] as it is strictly for $z\neq 0$: the appearance of contract terms beyond tree level renders the limit $z \rightarrow 0$ nonanalytic. On the contrary, the non-perturbative prescription of the previous section can be applied for any value of z , as the calculation is performed on each z separately. The values of Fig. 1 will be used in the following section to bring the RI' non-perturbative Z -factors to the $\overline{\text{MS}}$ scheme.

3 Results

Here we apply the prescription suggested in the previous Section and we present our results for the non-perturbative Z -factors both in the RI' and the $\overline{\text{MS}}$ schemes. For demonstration purposes we focus on the data with 5 steps of HYP smearing that suppress the power divergence and bring the results closer to renormalized nucleon matrix elements. We mainly focus on the multiplicative renormalization for the helicity quasi-PDFs. Furthermore, we have applied the two values of the RI' scale $\bar{\mu}_0$ that are shown in Fig. 1 (“parallel” and “diagonal”). After converting to the $\overline{\text{MS}}$ scheme at the same scale $\bar{\mu}=2$ GeV we can quantify their lattice artifacts, as explained below.

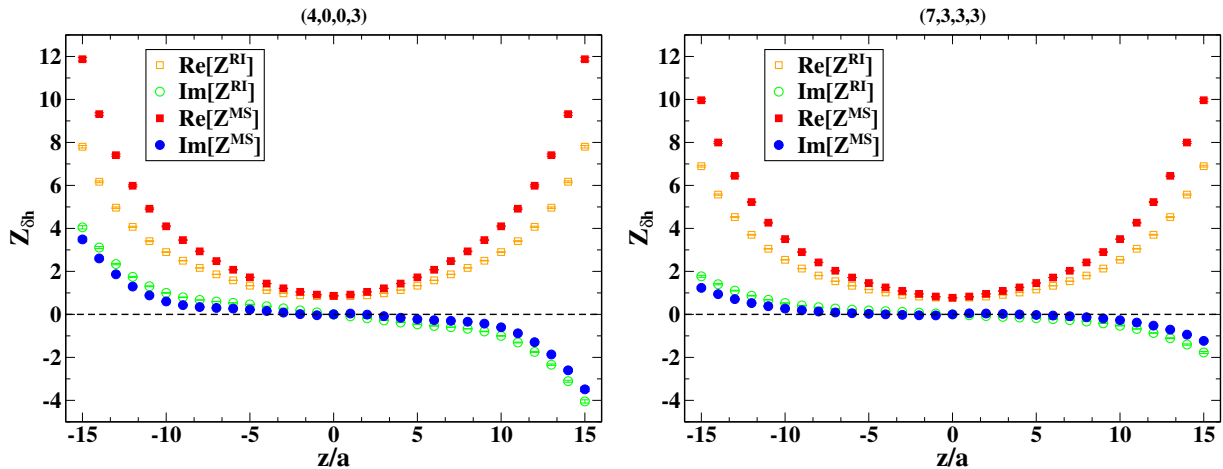


Figure 2: The z -dependent renormalization function for the matrix element $\delta h(P_3, z)$ with $P_3 = \frac{6\pi}{L}$. The “parallel” and “diagonal” choices for $\vec{\mu}_0$ are shown in the left and right plots, respectively. Open (filled) symbols correspond to the RI' ($\overline{\text{MS}}$) estimates.

In Fig. 2, we show the extracted values for the helicity Z -factor, $Z_{\delta h}$, that renormalizes

the bare matrix element $\delta h(P_3, z)$ for $P_3 = \frac{6\pi}{L}$. In each plot we overlay the results for the RI' (open symbols) and the $\overline{\text{MS}}$ (filled symbols) schemes, for the real and imaginary part of the Z -factor. We employ the momentum source technique [41, 34] that offers high statistical accuracy with a small number of measurements, typically of $\mathcal{O}(10)$. As can be seen in the plots, the statistical uncertainties are almost invisible. The left (right) plot corresponds to the “parallel” (“diagonal”) choices for $\bar{\mu}_0$.

We remind the reader that $Z_{\delta m}^{\text{RI}}$ depends on the RI' scale, which is different for the two plots we show in Fig. 2. However, upon conversion to the $\overline{\text{MS}}$ scheme and the evolution to 2 GeV, one should be able to compare the values for $Z_{\delta m}^{\overline{\text{MS}}}$. Thus, the filled symbols of same color in the two plots may be quantitatively compared. The difference between the two is an indication of the presence of lattice artifacts, mainly in the “parallel” case. This is demonstrated in Fig. 3 for both the real and imaginary parts, and it is interesting to see that the difference increases as z becomes larger. Based on this observation, we expect that such an increase of the lattice artifacts is also present for the “diagonal” case, but less severe. Thus, we conclude that the lattice artifacts must be addressed, in order to extract reliable estimates on the renormalization functions.

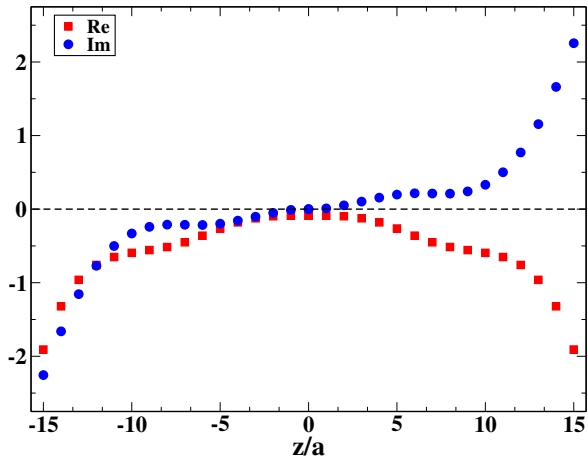


Figure 3: Difference of $Z_{\delta m}^{\overline{\text{MS}}}$ between the “parallel” and “diagonal” cases for $\bar{\mu}_0$. The real and imaginary parts are shown with red squares and blue circles, respectively.

We find that the imaginary part of $Z_{\delta m}^{\overline{\text{MS}}}$ is reduced compared to its counterpart in $Z_{\delta m}^{\text{RI}}$, and is also rather small for low values of z . This is more pronounced in the right plot of Fig. 2 for “diagonal” $\bar{\mu}_0$, for which $\text{Im}[Z_{\delta m}^{\overline{\text{MS}}}]$ (blue circles) is smaller than the corresponding data from the “parallel” scale, especially for large values of z . It is worth mentioning that the perturbative Z -factor in dimensional regularization and in the $\overline{\text{MS}}$ scheme is real to all orders in perturbation theory, as it is extracted only from the poles. Therefore, it is expected that the imaginary part of the non-perturbative estimates should be highly suppressed. The behavior of the “diagonal” scale is encouraging, as the imaginary part is very close to zero for $|z|$ up to $\sim 10a$. The residual imaginary part -mostly at large values of z as shown in Fig. 2- is an indication of two effects:

- a. important two-loop contributions to the conversion factor, and
- b. large lattice artifacts at high values of z/a .

It is our intention to address both effects in the near future, which will eliminate systematic uncertainties propagated to the estimates of the quasi-PDFs. Understanding the uncertainties dominating the large- z region is crucial, as the matrix element for these values also enters in

the Fourier transformation that yields the quasi-PDF. Preliminary explorations indicate that a likely magnitude of the two-loop contribution might suppress the imaginary part of $Z_{\delta m}^{\overline{\text{MS}}}$. However, we are currently in no position to quantify the systematics due to the truncation of the conversion factor.

At $z=0$ the aforementioned Z -factor is scheme- and scale-independent and corresponds to the renormalization functions of the axial current, Z_A , previously evaluated for this ensemble in Ref. [34]. In the latter calculation several diagonal scales have been employed and, together with a technique for the removal of the lattice artifacts, the extracted value was found to be $Z_A=0.7556(5)$. In the present calculation at $z=0$ we find a value of $Z_A\sim 0.86$ using the scale $\bar{\mu}_0=\frac{2\pi}{32}(\frac{4}{2}+\frac{1}{4},0,0,3)$, and $Z_A\sim 0.77$ for the scale $\bar{\mu}_0=\frac{2\pi}{32}(\frac{7}{2}+\frac{1}{4},3,3,3)$. This is yet another indication that lattice artifacts are large for the “parallel” renormalization scale and less severe, but not negligible, for the “diagonal” case.

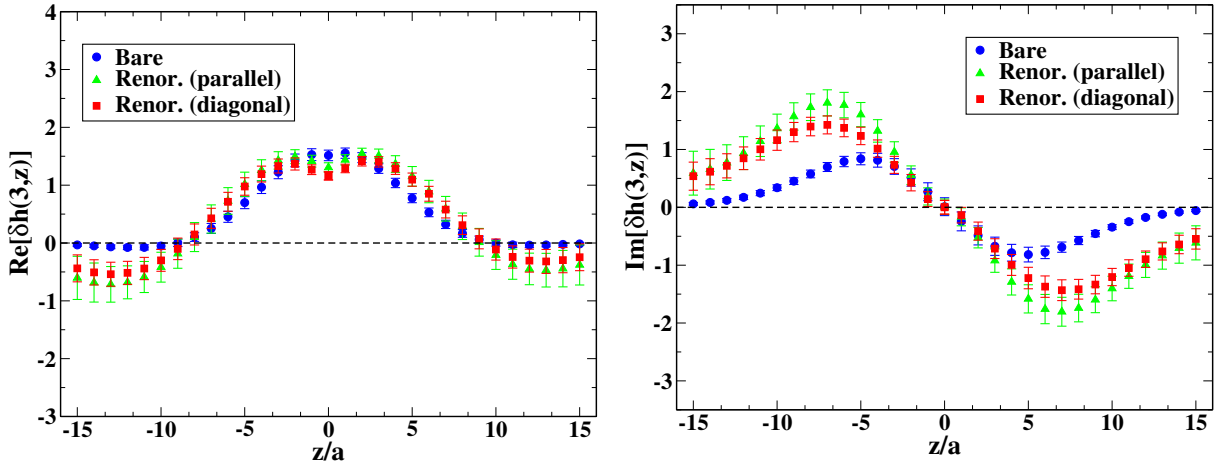


Figure 4: Renormalized matrix elements for the helicity quasi-PDF in the $\overline{\text{MS}}$ at $\bar{\mu}=2$ GeV, starting from the “parallel” RI’ scale, abbreviated as (4,0,0,3).

In Fig. 4, we show the renormalized helicity nucleon matrix elements using $Z_{\delta m}^{\overline{\text{MS}}}$ extracted from the two types of the RI’ scale. This is a straightforward procedure as there is no mixing for the axial operator and, therefore, the renormalization is only multiplicative. Such a plot is presented here for the first time, and it demonstrates the enormous progress in the field of the quasi-PDFs. However, before attempting to compare with the physical PDFs, we must understand the uncertainties related to the renormalization functions. In fact, we observe several interesting features of the lattice data, indicating the need for further investigation of the various sources of systematics. Below we summarize the main points:

1. At $z=0$, the obtained value of Z_A from the “parallel” scale is $\sim 15\%$ higher than the value obtained in Ref. [34]. If one employs the “diagonal” scale, then Z_A is only $\sim 3\%$ higher. This gives an indication that diagonal choices for the RI’ scale are preferable. A rule of thumb for the choice of $\bar{\mu}_0$ is that the ratio \hat{P} ($\equiv \frac{\sum_p \bar{\mu}_0^4 p}{(\sum_p \bar{\mu}_0^2 p)^2}$) takes a small value, typically $\hat{P} < 0.35$. In the values chosen for $P_3=\frac{6\pi}{L}$ we find: $\hat{P}=0.25$ for the the diagonal “(7,3,3,3)” and $\hat{P}=0.5$, while for the parallel “(4,0,0,3)”. The use of renormalization scales with large ratio \hat{P} induces large discretization effects, as can be seen e.g. in Fig. 15 of Ref. [34], representing the residual dependence of Z_A on initial RI’ scale for the local current. However, scales with $\hat{P} > 0.4$ may be included in the analysis, provided that the lattice artifacts are computed explicitly in lattice perturbation theory and subtracted in a process that follows closely Ref. [34]. We believe that the local minimum observed at

$z=0$ is a consequence of large cut-off effects, which we expect will be smoothed out upon subtraction of $\mathcal{O}(g^2 a^\infty)$ lattice artifacts.

2. As z increases there is an amplification of the imaginary part of the nucleon matrix element, in particular for $z/a \gtrsim 10$. This effect might have resulted from the truncation of the conversion factor (only one-loop result is known), and/or significant artifacts for large- z Wilson lines. As previously mentioned, we observe a sizable imaginary part of $Z_{\delta m}^{\overline{\text{MS}}}$ for $z/a \gtrsim 5$, indicating that the truncation of the conversion factor at one-loop level induces numerically large effects. In particular, the real part of the renormalized matrix element,

$$\text{Re} [\delta h^{ren}] = \text{Re} [Z_{\delta m}^{\overline{\text{MS}}}] \text{Re} [\delta h^{bare}] - \text{Im} [Z_{\delta m}^{\overline{\text{MS}}}] \text{Im} [\delta h^{bare}] \quad (16)$$

receives negative contributions from the imaginary part of the bare matrix element if $Z_{\delta m}^{\overline{\text{MS}}}$ has a non-zero imaginary part and $\text{Im} \delta h^{bare}$ decays to zero more slowly than $\text{Re} \delta h^{bare}$, which is what we observe in the data. Likewise, the large- z region of the imaginary part of the renormalized matrix element

$$\text{Im} [\delta h^{ren}] = \text{Re} [Z_{\delta m}^{\overline{\text{MS}}}] \text{Im} [\delta h^{bare}] + \text{Im} [Z_{\delta m}^{\overline{\text{MS}}}] \text{Re} [\delta h^{bare}] \quad (17)$$

is also affected by the non-zero imaginary part of $Z^{\overline{\text{MS}}}$.

4 Conclusions - Discussion

In this work we have presented a concrete prescription to renormalize non-perturbatively the matrix elements needed for the computation of quasi-PDFs. The employed scheme is RI', which is then converted to the $\overline{\text{MS}}$ scheme and evolved to 2 GeV; this is done perturbatively to one-loop. We have argued that the renormalization condition properly handles both kinds of divergences present in the matrix elements: the standard logarithmic divergence and the power divergence specific to non-local operators containing a Wilson line. Furthermore, we provide the renormalization conditions to eliminate the mixing in the case of the unpolarized quasi-PDFs that mixes with the twist-3 scalar operator.

We have also demonstrated the implementation of the proposed prescription to the helicity quasi-PDFs and presented the corresponding renormalized matrix elements. This has allowed us to draw conclusions how to make the computation more robust, which is the main outcome of this work.

- First, an essential ingredient of a computation with controlled systematic uncertainties is the subtraction of one-loop lattice artifacts in the framework of lattice perturbation theory. Following the ideas of Ref. [34], we are currently computing the $\mathcal{O}(g^2 a^\infty)$ artifacts that will be subtracted from the non-perturbative estimates for the Z -factors. In this way, the presence of large cut-off effects in the renormalized functions (especially for “parallel” momenta) will be avoided to a large extent.
- Second, the conversion factor from the RI' renormalization scheme to the $\overline{\text{MS}}$ scheme is likely to have sizable higher order corrections that, among others, are responsible for the unphysical feature of the real part of the renormalized matrix element becoming negative for large Wilson line lengths. A two-loop computation of this conversion factor is expected to resolve this issue to a sufficient degree. We have performed numerical experiments that indicate that a natural change of the conversion factor by two-loop contributions, i.e. around 10-20% (which is approximately α_s at the considered scale), should be enough to suppress the unwanted effect. A perturbative calculation of the conversion factor to two loops is quite laborious and will be presented separately.

To summarize, the renormalization program presented in this work together with future improvements that are being pursued, will provide reliable estimates for the renormalization functions of the Wilson line fermion operators. In this fashion, the obtained renormalized matrix elements can be used as an input to calculate the quasi-PDFs and match them to light-front PDFs, which is the main aim of the whole approach. Apart from the helicity case discussed in this work, we will address the transversity PDF in an analogous manner. For the unpolarized case, one needs to take into account the mixing with the scalar operator, as explained here. With this work, we have proposed and discussed a complete renormalization program of the quasi-PDFs, which has been a major uncertainty prior to this work and constitutes a major milestone in connecting lattice QCD results to the light-cone PDFs.

Acknowledgements

We would like to thank the members of ETMC for useful and fruitful discussions. We also thank Rainer Sommer for discussions related to the arbitrary scale in the renormalization prescription. KC was supported in part by the Deutsche Forschungsgemeinschaft (DFG), project nr. CI 236/1-1. MC acknowledges financial support by the U.S. Department of Energy, Office of Science, Office of Nuclear Physics, within the framework of the TMD Topical Collaboration. We acknowledge funding from the European Union’s Horizon 2020 research and innovation program under the Marie Skłodowska-Curie grant agreement No 642069.

References

- [1] R. P. Feynman, Photon-Hadron Interactions, *Frontiers in Physics*, Benjamin, Reading, MA, 1972.
- [2] M. Constantinou, Hadron Structure, *PoS LATTICE2014* (2014) 001. [arXiv:1411.0078](#).
- [3] M. Constantinou, Recent progress in hadron structure from Lattice QCD, *PoS CD15* (2015) 009. [arXiv:1511.00214](#).
- [4] C. Alexandrou, K. Jansen, Hadron structure from lattice QCD, *Nucl. Part. Phys. Proc.* 261-262 (2015) 202–217.
- [5] C. Alexandrou, Selected results on hadron structure using state-of-the-art lattice qcd simulations, in: *Proceedings, 45th International Symposium on Multiparticle Dynamics (ISMD 2015)*: Kreuth, Germany, October 4-9, 2015, 2015. [arXiv:1512.03924](#).
- [6] S. Syritsyn, Review of Hadron Structure Calculations on a Lattice, *PoS LATTICE2013* (2014) 009. [arXiv:1403.4686](#).
- [7] P. Jimenez-Delgado, W. Melnitchouk, J. F. Owens, Parton momentum and helicity distributions in the nucleon, *J. Phys. G40* (2013) 093102. [arXiv:1306.6515](#).
- [8] A. Accardi, L. T. Brady, W. Melnitchouk, J. F. Owens, N. Sato, Constraints on large- x parton distributions from new weak boson production and deep-inelastic scattering data, *Phys. Rev. D93* (11) (2016) 114017. [arXiv:1602.03154](#).
- [9] S. Alekhin, J. Blaumlein, S. Moch, R. Placakyte, Parton Distribution Functions, α_s and Heavy-Quark Masses for LHC Run II [arXiv:1701.05838](#).
- [10] X. Ji, Parton Physics on a Euclidean Lattice, *Phys.Rev.Lett.* 110 (2013) 262002. [arXiv:1306.1539](#).
- [11] X. Xiong, X. Ji, J.-H. Zhang, Y. Zhao, One-loop matching for parton distributions: Non-singlet case, *Phys.Rev. D90* (1) (2014) 014051. [arXiv:1310.7471](#).
- [12] J.-W. Chen, X. Ji, J.-H. Zhang, Improved quasi parton distribution through Wilson line renormalization, *Nucl. Phys. B915* (2017) 1–9. [arXiv:1609.08102](#).
- [13] H.-W. Lin, J.-W. Chen, S. D. Cohen, X. Ji, Flavor Structure of the Nucleon Sea from Lattice QCD, *Phys. Rev. D91* (2015) 054510. [arXiv:1402.1462](#).
- [14] L. Gamberg, Z.-B. Kang, I. Vitev, H. Xing, Quasi-parton distribution functions: a study in the diquark spectator model, *Phys. Lett. B743* (2015) 112–120. [arXiv:1412.3401](#).
- [15] C. Alexandrou, K. Cichy, V. Drach, E. Garcia-Ramos, K. Hadjyiannakou, K. Jansen, F. Steffens, C. Wiese, Lattice calculation of parton distributions, *Phys. Rev. D92* (1) (2015) 014502. [arXiv:1504.07455](#).
- [16] J.-W. Chen, S. D. Cohen, X. Ji, H.-W. Lin, J.-H. Zhang, Nucleon Helicity and Transversity Parton Distributions from Lattice QCD, *Nucl. Phys. B911* (2016) 246–273. [arXiv:1603.06664](#).
- [17] C. Alexandrou, K. Cichy, M. Constantinou, K. Hadjyiannakou, K. Jansen, F. Steffens, C. Wiese, New Lattice Results for Parton Distributions, [arXiv:1610.03689](#).
- [18] A. Radyushkin, Target Mass Effects in Parton Quasi-Distributions, *Phys. Lett. B770* (2017) 514–522. [arXiv:1702.01726](#).
- [19] A. Radyushkin, Nonperturbative Evolution of Parton Quasi-Distributions, *Phys. Lett. B767* (2017) 314–320. [arXiv:1612.05170](#).

- [20] V. S. Dotsenko, S. N. Vergeles, Renormalizability of Phase Factors in the Nonabelian Gauge Theory, *Nucl. Phys.* B169 (1980) 527–546.
- [21] M. Constantinou, H. Panagopoulos, Perturbative Renormalization of quasi-PDFs, [arXiv:1705.11193](https://arxiv.org/abs/1705.11193).
- [22] Y.-Q. Ma, J.-W. Qiu, Extracting Parton Distribution Functions from Lattice QCD Calculations, [arXiv:1404.6860](https://arxiv.org/abs/1404.6860).
- [23] T. Ishikawa, Y.-Q. Ma, J.-W. Qiu, S. Yoshida, Practical quasi parton distribution functions, [arXiv:1609.02018](https://arxiv.org/abs/1609.02018).
- [24] C. Monahan, K. Orginos, Quasi parton distributions and the gradient flow, *JHEP* 03 (2017) 116. [arXiv:1612.01584](https://arxiv.org/abs/1612.01584).
- [25] G. Martinelli, C. Pittori, C. T. Sachrajda, M. Testa, A. Vladikas, A General method for nonperturbative renormalization of lattice operators, *Nucl.Phys.* B445 (1995) 81–108. [arXiv:hep-lat/9411010](https://arxiv.org/abs/hep-lat/9411010).
- [26] R. Baron, P. Boucaud, J. Carbonell, A. Deuzeman, V. Drach, et al., Light hadrons from lattice QCD with light (u,d), strange and charm dynamical quarks, *JHEP* 1006 (2010) 111. [arXiv:1004.5284](https://arxiv.org/abs/1004.5284).
- [27] N. Carrasco, et al., Up, down, strange and charm quark masses with $N_f = 2+1+1$ twisted mass lattice QCD, *Nucl. Phys.* B887 (2014) 19–68. [arXiv:1403.4504](https://arxiv.org/abs/1403.4504).
- [28] R. Sommer, Non-perturbative Heavy Quark Effective Theory: Introduction and Status, *Nucl. Part. Phys. Proc.* 261-262 (2015) 338–367. [arXiv:1501.03060](https://arxiv.org/abs/1501.03060).
- [29] C. Alexandrou, M. Constantinou, T. Korzec, H. Panagopoulos, F. Stylianou, Renormalization constants for 2-twist operators in twisted mass QCD, *Phys. Rev.* D83 (2011) 014503. [arXiv:1006.1920](https://arxiv.org/abs/1006.1920).
- [30] M. Constantinou, et al., Non-perturbative renormalization of quark bilinear operators with $N_f = 2$ (tmQCD) Wilson fermions and the tree-level improved gauge action, *JHEP* 08 (2010) 068. [arXiv:1004.1115](https://arxiv.org/abs/1004.1115).
- [31] A. Abdel-Rehim, et al., Simulating QCD at the Physical Point with $N_f = 2$ Wilson Twisted Mass Fermions at Maximal Twist, [arXiv:1507.05068](https://arxiv.org/abs/1507.05068).
- [32] A. Abdel-Rehim, et al., Nucleon and pion structure with lattice QCD simulations at physical value of the pion mass, *Phys. Rev.* D92 (11) (2015) 114513. [arXiv:1507.04936](https://arxiv.org/abs/1507.04936).
- [33] M. Constantinou, R. Horsley, H. Panagopoulos, H. Perlt, P. E. L. Rakow, G. Schierholz, A. Schiller, J. M. Zanotti, Renormalization of local quark-bilinear operators for $N_f=3$ flavors of stout link nonperturbative clover fermions, *Phys. Rev.* D91 (1) (2015) 014502. [arXiv:1408.6047](https://arxiv.org/abs/1408.6047).
- [34] C. Alexandrou, M. Constantinou, H. Panagopoulos, Renormalization functions for $N_f=2$ and $N_f=4$ twisted mass fermions, *Phys. Rev.* D95 (3) (2017) 034505. [arXiv:1509.00213](https://arxiv.org/abs/1509.00213).
- [35] A. J. Buras, P. H. Weisz, QCD Nonleading Corrections to Weak Decays in Dimensional Regularization and 't Hooft-Veltman Schemes, *Nucl. Phys.* B333 (1990) 66–99.
- [36] A. Patel, S. R. Sharpe, Perturbative corrections for staggered fermion bilinears, *Nucl. Phys.* B395 (1993) 701–732. [arXiv:hep-lat/9210039](https://arxiv.org/abs/hep-lat/9210039).
- [37] S. A. Larin, J. A. M. Verma, The Three loop QCD Beta function and anomalous dimensions, *Phys. Lett.* B303 (1993) 334–336. [arXiv:hep-ph/9302208](https://arxiv.org/abs/hep-ph/9302208).
- [38] S. A. Larin, The Renormalization of the axial anomaly in dimensional regularization, *Phys. Lett.* B303 (1993) [See also hep-ph/9302240 for an additional Section] 113–118. [arXiv:hep-ph/9302240](https://arxiv.org/abs/hep-ph/9302240).

- [39] A. Skouroupathis, H. Panagopoulos, Two-loop renormalization of vector, axial-vector and tensor fermion bilinears on the lattice, *Phys. Rev. D* 79 (2009) 094508. [arXiv:0811.4264](https://arxiv.org/abs/0811.4264).
- [40] M. Constantinou, M. Costa, H. Panagopoulos, Perturbative renormalization functions of local operators for staggered fermions with stout improvement, *Phys. Rev. D* 88 (2013) 034504. [arXiv:1305.1870](https://arxiv.org/abs/1305.1870).
- [41] M. Gockeler, R. Horsley, H. Oelrich, H. Perlt, D. Petters, P. E. L. Rakow, A. Schafer, G. Schierholz, A. Schiller, Nonperturbative renormalization of composite operators in lattice QCD, *Nucl. Phys. B* 544 (1999) 699–733. [arXiv:hep-lat/9807044](https://arxiv.org/abs/hep-lat/9807044).